Optical spectroscopy of X-Mega targets – II. The massive double-lined O-type binary HD 93205

N. I. Morrell,[1]★† R. H. Barbá,[1]† V. S. Niemela,[1]‡ M. A. Corti,[1]§ J. F. Albacete Colombo,[1] G. Rauw,[2]¶ M. Corcoran,[3,4] T. Morel,[5] J.-F. Bertrand,[6] A. F. J. Moffat[6] and N. St-Louis[6]

[1]*Facultad de Ciencias Astronómicas y Geofísicas, Universidad Nacional de La Plata, Paseo del Bosque S/N, B1900FWA La Plata, Argentina*
[2]*Institut d'Astrophysique et de Géophysique, Université de Liège, 5, Avenue de Cointe, B 4000 Liège, Belgium*
[3]*Universities Space Research Association, 7501 Forbes Blvd, Ste 206, Seabrook, MD 20706, USA*
[4]*Laboratory for High Energy Astrophysics, Goddard Space Flight Center, Greenbelt, MD 20771, USA*
[5]*Inter-University Center for Astronomy and Astrophysics (IUCAA), Post Bag 4, Ganeshkhind, Pune 411 007, India*
[6]*Département de Physique, Université de Montréal, and Observatoire du Mont Mégantic, CP 6128, Succursale Centre-ville, Montréal,QC H3C 3J7, Canada*

ABSTRACT

A new high-quality set of orbital parameters for the O-type spectroscopic binary HD 93205 has been obtained combining échelle and coudé CCD observations. The radial velocity orbits derived from the He II $\lambda 4686$ Å (primary component) and He I $\lambda 4471$ Å (secondary component) absorption lines yield semi-amplitudes of 133 ± 2 and 314 ± 2 km s^{-1} for each binary component, resulting in minimum masses of 31 and 13 M$_\odot$ ($q = 0.42$). We also confirm for the binary components the spectral classification of O3 V + O8 V previously assigned. Assuming for the O8 V component a 'normal' mass of 22–25 M$_\odot$ we would derive for the primary O3 V a mass of 'only' 52–60 M$_\odot$ and an inclination of about 55° for the orbital plane. We have also determined for the first time a period of apsidal motion for this system, namely 185 ± 16 yr using all available radial velocity data sets of HD 93205 (from 1975 to 1999). Phase-locked variations of the X-ray emission of HD 93205 consisting of a rise of the observed X-ray flux near periastron passage are also discussed.

Key words: binaries: general – stars: early-type – stars: individual: HD 93205 – X-rays: stars.

1 INTRODUCTION

The Carina Nebula region is known to harbour some of the youngest and most massive O-type stars in our galaxy (cf. Walborn 1995). This region, containing the open clusters Trumpler 14, Trumpler 16 and Collinder 228, is indeed the major concentration of O-type stars known in the nearby Milky Way. Hot stars are frequently observed as X-ray sources, though the mechanism responsible for this emission still remains poorly understood. While X-ray emission can arise from the winds of hot single stars, the binary nature of some of them might also contribute to X-ray production through wind–wind collision effects. In general, the ratio between X and bolometric luminosities (L_x/L_{bol}) seems to be close to 10^{-7} for OB stars (Corcoran 1999), but the proposed relation exhibits a large scatter. With the aim of addressing some of those problems, in late 1995, the X-Mega collaboration (Corcoran

et al. 1999) started observations and analysis of X-ray emission from hot massive stars. Obviously, the Carina Nebula was one of its first selected targets.

In the first paper of this series (Albacete Colombo, Morrell & Niemela 2001) we reported the discovery of a new double-lined O-type binary among the members of the open cluster Trumpler 16. Another O-type member of Trumpler 16, HD 93205, is the only O3 V star in the Milky Way known to belong to a double-lined binary system (Walborn 1971, 1973). Although similar systems have been recently discovered in the Large Magellanic Cloud (LMC) (e.g. Massey & Hunter 1998; Bertrand, St-Louis & Moffat 1998), HD 93205 is still the earliest type star in our Galaxy for which an orbital solution is available. This makes this system specially valuable for the mass–luminosity relation for the most massive stars.

Conti & Walborn (1976, hereafter CW76) classified the binary components of HD 93205 as O3 V + O8 V and presented the first radial velocity orbit for this system, deriving a period of 6.0810 ± 0.0007 d and minimum masses of 39 and 15 M$_\odot$ respectively. They found a highly eccentric orbit ($e = 0.49$) which also suggests that this system is extremely young, with both components very close to the zero-age main sequence (ZAMS). Subsequent radial velocity studies by Levato et al. (1991) and Stickland & Lloyd (1993,

★E-mail: nidia@fcaglp.unlp.edu.ar
† Member of Carrera del Investigador Científico, CONICET, Argentina.
‡ Member of Carrera del Investigador Científico, CIC, Prov. de Buenos Aires, Argentina.
§ Fellow of FOMEC.
¶ Postdoctoral Researcher FNRS (Belgium).

Table 1. Instrumental configurations for different observing runs.

Id.	Date	Observat.	Tel.	Spectrogr.	CCD	$\lambda/\Delta(\lambda)$	Spec. Range [Å]	No. Obs.
1	Jan. 1995	CASLEO	2.15-m	REOSC	Tek 1024	7500	3500–6000	4
2	Jan. 1995	UTSO	0.6-m	Garrison	PM 512	1000	4000–5000	9
3	Feb. 1997	CASLEO	2.15-m	REOSC	Tek 1024	15000	3500–6000	15
4	March 1997	ESO	1.5-m	B&C	ESO CCD#39	3000	3850–4800	6
5	June 1997	ESO	1.4-m	CAT CES	ESO CCD#38	70000	4445–4495	5
6	Dec. 1997	CASLEO	2.15-m	B&C	PM 512	1000	3900–5000	2
7	Jan.–Feb. 1998	CASLEO	2.15-m	REOSC	Tek 1024	15000	3500–6000	12
8	Feb. 1998	CASLEO	2.15-m	B&C	PM 512	1000	3900–5000	2
9	July 1998	ESO	1.4-m	CAT CES	ESO CCD#38	70000	4461–4480	5
10	Jan.–Feb. 1999	CASLEO	2.15-m	REOSC	Tek 1024	15000	3500–6000	8

hereafter SL93) essentially confirmed the preliminary results by CW76.

The first observational efforts aimed at the search for photometric variability in HD 93205 (van Genderen et al. 1985a,b, 1989) showed only marginal evidence for light variations. Then, Antokhina et al. (2000) found clear phase-dependent variations with full amplitude ~0.02 mag in visual light. These are probably related to tidal distortions rather than eclipses, leaving room for a wide range of possible orbital inclinations, $35° < i < 75°$, with most likely value $i = 60°$. The relatively low values derived for the minimum masses of the binary components also support the idea that the inclination is not very high.

Several studies considered the mass ratio ($q \sim 0.4$) of the HD 93205 binary system to be 'anomalous' (e.g. SL93; Penny, Gies & Bagnuolo 1998). This statement is based on the assumption that the secondary, an O8 V star, has a mass of $\sim 25\,M_\odot$, as suggested by both binary star observations (cf. Schönberner & Harmanec 1995; Burkholder, Massey & Morrell 1997) and evolutionary tracks (cf. Schaller et al. 1992). Then the mass of the O3 V star would be 'only' $\sim 60\,M_\odot$, much lower than the expected value, based on evolutionary tracks.

Taking into account that HD 93205 is, in our Galaxy, the only well-studied binary system containing an O3 V-type non-evolved component, and in view of the apparent discrepancy between the observed mass ratio and that predicted by the evolutionary models, we decided to perform a new study mainly based on high-resolution CCD spectroscopic observations of this key binary system. Moreover, HD 93205 is, as mentioned above, one of the Carina targets observed in the context of the X-Mega campaign, and a new orbital determination was advisable in order to plan and interpret the X-ray observations.

2 OBSERVATIONS

The present study is the result of a collaboration in which several data sets were obtained at three different southern observatories, using four telescopes and five spectrographs. Table 1 lists details of each instrumental configuration.

39 CCD échelle spectra of HD 93205 were obtained at the Complejo Astronómico El Leoncito, Argentina (CASLEO)[1] between 1995 and 1999 with the 2.15-m Jorge Sahade Telescope. We used a REOSC échelle Cassegrain spectrograph and a Tek 1024×1024 pixel CCD as detector to obtain 35 spectra in the approximate wavelength range 3500 to 6000 Å, at a reciprocal

dispersion of 0.17 Å pixel^{-1} at 4500 Å. Four échelle spectra of HD 93205 were obtained at CASLEO in 1995 January with the configuration described above but binning the CCD by a factor of 2. Four additional observations were obtained at CASLEO with a Boller & Chivens (B&C) spectrograph attached to the 2.15-m telescope, using a PM 512×512 CCD as detector, and a 600 line mm^{-1} diffraction grating, yielding a reciprocal dispersion of 2.5 Å pixel^{-1}.

16 CCD spectra of HD 93205 were obtained at the European Southern Observatory (ESO) in Chile. Six of them were gathered with the B&C spectrograph attached to the 1.5-m telescope, at a reciprocal dispersion of 0.6 Å pixel^{-1} covering the wavelength region from 3850 to 4800 Å. The detector was a thinned, UV-flooded CCD (ESO ccd#39) and the spectral resolution as measured from the full width at half-maximum (FWHM) of the lines of the helium–argon calibration spectra was 1.1 Å. Ten spectra were obtained with the 1.4-m Coudé Auxiliary Telescope (CAT), using the Coudé Echelle Spectrometer equipped with the Long Camera (LC) in 1997 and the Very Long Camera (VLC) in 1998. The detector used during both runs was a Loral 2688×512 pixel CCD with a pixel size of 15 μm × 15 μm. The effective resolving power as derived from the FWHM of the lines of the ThAr calibration exposures was 70 000. Typical exposure times were of the order of 30–45 min. The wavelength domain was centred at $\lambda\,4470$ Å, and covered a narrow spectral window of 40 Å for the LC and 20 Å for the VLC.

Nine CCD spectra were obtained with the Cassegrain spectrograph attached to the 0.6-m telescope at the University of Toronto Southern Observatory (UTSO), Chile. These data, obtained with a 600 line mm^{-1} grating blazed at 4700 Å in first order, cover the blue region of the spectrum at a reciprocal dispersion of 2 Å pixel^{-1}. Consecutive exposures were combined in order to obtain one radial velocity determination for each observing night, as shown in Table 2.

The usual sets of bias and flat-fields were also secured for each observing night.

Data from CASLEO and UTSO were reduced and analysed with IRAF[2] routines, while MIDAS[3] software was used for the reductions and analysis of data obtained at ESO.

3 RADIAL VELOCITIES

One of our goals being the determination of an accurate radial velocity orbit for the HD 93205 binary system, we decided to use

---

[1] CASLEO is operated under agreement between CONICET and the National Universities of La Plata, Córdoba and San Juan.

[2] IRAF is distributed by NOAO, operated by AURA, Inc., under agreement with NSF.

[3] MIDAS is developed and maintained by the European Southern Observatory.

Table 2. Low-dispersion radial velocities of HD 93205.

HJD 2 400 000+	Phase ϕ	O3 V Star [km s^{-1}]	O8 V Star [km s^{-1}]	Run
49732.745	0.963	$122 \pm 6(2)$	$-326 \pm 45(2)$	2
49733.622	0.108	$-37 \pm 7(3)$	$100 \pm 21(3)$	2
49734.728	0.289	$-107 \pm 5(3)$	$202 \pm 12(3)$	2
49736.697	0.613	$8 \pm 9(3)$	$33 \pm 11(3)$	2
49737.706	0.779	$76 \pm 12(3)$	$-150 \pm 39(3)$	2
49738.715	0.945	$191 \pm 7(3)$	$-285 \pm 38(3)$	2
49742.695	0.600	$6 \pm 22(3)$	$69 \pm 11(3)$	2
49743.672	0.760	$60 \pm 7(3)$	$-119 \pm 14(3)$	2
49744.674	0.925	$221 \pm 10(3)$	$-375 \pm 22(3)$	2
50534.666	0.852	$145 \pm 2(3)$	$-294 \pm 36(3)$	4
50535.661	0.015	$81 \pm 12(3)$	$-191 \pm 31(3)$	4
50536.656	0.179	$-108 \pm 16(3)$	$219 \pm 19(3)$	4
50537.687	0.349	$-93 \pm 8(3)$	$224 \pm 15(3)$	4
50538.652	0.507	$-57 \pm 1(2)$	$38(1)$	4
50539.653	0.672	$-16 \pm 4(2)$	$-55(1)$	4
50807.844	0.780	$-19 \pm 19(3)$	$-211(1)$	6
50811.872	0.443	$-92 \pm 27(3)$	$58(1)$	6
50858.819	0.164	$-98 \pm 12(3)$	$148 \pm 15(2)$	8
50861.831	0.659	$-19 \pm 13(3)$	$-112 \pm 11(2)$	8

Notes: The meaning of the columns are as follows: (1) Heliocentric Julian Date; (2) orbital phase computed with the new ephemeris (see Section 4); (3) heliocentric radial velocity of the primary component; (4) heliocentric radial velocity of the secondary component; (5) observing run identification. Quoted errors are standard deviations of the mean derived from the average of several spectra obtained in succesive exposures (between parenthesis) in Run 2, and from the average of several absorption lines (between parenthesis) in each spectrum for Runs 4, 6 and 8.

only the high-resolution CCD observations for that purpose. However, all the available spectroscopic observations, either newly obtained or previously published, were used in the analysis, leading to a determination of the period of apsidal motion.

Table 2 shows the journal of our low-resolution observations. These radial velocities were obtained through simple Gaussian fitting to the observed He I and He II absorption line profiles, considering that the major contributor to the former is the O8 secondary star, while He II lines mainly originate in the primary O3 component.

Table 3 presents the journal of our high-resolution observations. Again, orbital phases were computed with the new ephemeris. We list heliocentric radial velocities measured for He I λ4471.479 Å and He II λ4685.682 Å for both binary components. Depending on the degree of blending, we applied simple or simultaneous double Gaussian fitting to the absorption-line profiles, in order to obtain the corresponding radial velocities. We selected these two lines for the radial velocity calculations, because they lie in a region of the CASLEO échelle spectra where highest signal-to-noise ratio (S/N) occurs. The He II line was better observed in the primary than in the secondary component, while the reversal is true for the He I line. In addition, He I 4471 Å is the only spectral line present in the CAT data set. For those cases where no double lines were observed, we attributed the He II line to the O3 V primary and the He I line to the O8 V secondary components, respectively. Fig. 1 displays the regions containing He II 4686 Å and He I 4471 Å absorption lines in several CASLEO high-resolution échelle spectrograms at four different phases of the binary period, illustrating the contribution of both binary components.

The stability of the radial velocity system for the CASLEO échelle data was checked in two ways: (i) by radial velocity measurements of nebular emission lines ([O III], [O II], and H I) present in the spectrum of HD 93205; and (ii) by measurement of several spectra of the constant radial velocity star HR 2806 for which we obtained a mean heliocentric radial velocity of 26 ± 1 km s^{-1} (standard deviation) in excellent agreement with other determinations (28.0 km s^{-1}, Garmany, Conti & Massey 1980; 25.9 km s^{-1}, Penny et al. 1993; 27.2 km s^{-1}, García et al. 1998). A typical internal standard deviation for our measurements of the radial velocity of HR 2806 is 4 km s^{-1}.

4 ORBITAL ELEMENTS AND THEIR DISCUSSION

4.1 The radial velocity orbit

The first determination of the orbital period of HD 93205 was performed by CW76, with a value of $P = 6.0810 \pm 0.0007$ d. Subsequent determinations by Levato et al. (1991) and SL93 gave values of $P = 6.08071 \pm 0.00007$ and $P = 6.08081 \pm 0.00007$ d, respectively, using all the radial velocity data available for the primary star at that moment. However the best period found by SL93 to fit the *IUE* data is $P = 6.0821 \pm 0.0004$ d. These authors also mention a possible apsidal motion with a period of about 400 yr, but the data then available were not enough for a conclusive result.

Apsidal motion changes the shape of a binary's radial velocity curve (in the elliptical case) when observed at different epochs. This effect in the orbit of HD 93205 is illustrated in Fig. 2, where each curve represents the best fit to the radial velocities of HD 93205 obtained during different years since the discovery of its binary nature, namely CW76, Levato et al. (1991), SL93, data from UTSO (this paper, 1995), CASLEO and ESO data (this paper, 1997–1999). We ploted each data set using the ephemeries derived from the last set (1997–1999).

In principle, apsidal motion also precludes the successful determination of the orbital period of a binary with the usual simple period searching techniques applied to radial velocity data gathered over several years. The fact that the various data sets have quite different qualities adds more confusion to this point. After some trials, which comprised the application of the Lafler & Kinman (1965) method and several subsequent modifications of it, e.g. Cincotta, Méndez & Núñez (1995), we concluded that we cannot attain for a simple determination with constant orbital parameters an accuracy higher than 0.0004 d for the period. We therefore adopted for the following calculations the most probable period derived from the high-resolution data sets, namely 6.0803 ± 0.0004 d.

We used for the determination of the radial velocity orbit of the HD 93205 system the He II 4686 and He I 4471 lines of both binary components measured from the high-resolution observations listed in Table 3. The orbital elements were obtained using a modified version of the code originally written by Bertiau & Grobben (1969), considering the radial velocity measurements for each binary component independently, or both binary components together.

The resulting orbital elements are listed in Table 4.

Fig. 3 shows the observed radial velocities along with the orbital solutions of Table 4 for He I 4471 Å and He II 4686 Å separately. Considering that the He II lines arise mainly in the O3 V primary component and He I is more representative of the secondary, we

Table 3. High-resolution radial velocity measurements for HD 93205.

HJD 2 400 000+	Phase ϕ	He I 4471 [km s^{-1}]					He II 4686 [km s^{-1}]					Run
		Prim.	$(O-C)_1$	Sec.	$(O-C)_1$	$(O-C)_3$	Prim.	$(O-C)_2$	$(O-C)_3$	Sec.	$(O-C)_2$	
49738.853	0.968	+138	−19	−337	+30	+26	+161	+14	+11	−338	+1	1
49739.855	0.133	−91	−6	+166	+11	+4	−64	+5	+9	+174	+11	1
49741.849	0.461	−91	−11	+150	+5	0	−56	+8	+12	+147	−6	1
49742.854	0.626			+31	+27	+20	+15	+16	+24			1
50494.863	0.305	−100	+19	+233	+8	+5	−97	+3	+4	+231	−6	3
50495.628	0.431	−96	−7	+169	+5	0	−70	+3	+6	+184	+11	3
50495.746	0.451			+153	+2	−4	−55	+12	+16	+137	−23	3
50495.864	0.470	−121	−44	+135	−3	−9	−49	+12	+16	+194	+48	3
50496.715	0.610			+33	+13	+6	+5	+13	+21			3
50497.751	0.780			−194	−5	−11	+81	0	+8	−193	−7	3
50497.864	0.799	+115	+27	−212	+5	0	+103	+10	+18			3
50498.599	0.920	+154	−12	−390	−4	−5	+162	+4	+3	−366	−3	3
50498.722	0.940	+141	−27	−378	+13	+12	+176	+18	+15	−387	−22	3
50498.852	0.961	+163	+2	−388	−12	−15	+151	0	−3	−340	+8	3
50505.659	0.081			+21	−8	−20	−10	+4	+12	+46	+9	3
50505.806	0.105			+108	+10	+1	−38	+6	+12			3
50506.610	0.237			+249	+17	+13	−91	+13	+13	+257	+12	3
50507.755	0.426	−48	+42	+174	+6	+2	−80	−6	−3	+179	+2	3
50508.614	0.567						−3	+23	+30			3
50622.519	0.300	−163	−46	+222	−4	−7						5
50623.538	0.468	−94	−17	+148	+8	+3						5
50624.496	0.626			−3	−7	−15						5
50625.530	0.796	+100	+15	−233	−21	−27						5
50626.499	0.955	+199	+34	−404	−21	−23						5
50841.720	0.351	−104	+5	+199	−8	−12	−95	−3	−1	+202	−17	7
50842.737	0.519			+85	−16	−23	−43	+1	+7	+95	−12	7
50843.804	0.694			−54	+18	+11	+9	−23	−14			7
50844.814	0.860	+108	−24	−343	−29	−32	+115	−17	−12	−300	+2	7
50845.792	0.021	+110	+28	−180	+25	+13	+76	−6	−1	−187	0	7
50846.797	0.186	−107	+5	+208	−7	−11	−104	−9	−7	+217	−9	7
50847.745	0.342	−108	+3	+182	−29	−33	−100	−6	−4	+236	+13	7
50848.806	0.517			+89	−14	−20	−24	+21	+27			7
50849.826	0.685			−50	+11	+4	+20	−7	+2	−64	−5	7
50850.819	0.848	+80	−43	−290	+4	+1	+127	+3	+8	−277	+8	7
50851.754	0.002			−278	+1	−8	+105	−7	−5	−259	−3	7
50852.805	0.175	−109	−1	+205	−1	−6	−99	−7	−5	+238	+21	7
50995.546	0.651			−23	−1	−8						9
50996.503	0.808	+103	+9	−232	−1	−6						9
50998.510	0.138	−113	−24	+168	+4	−2						9
50999.512	0.303	−125	−8	+228	+3	−1						9
51000.472	0.461	−87	−7	+157	+12	+7						9
51208.772	0.719			−87	+16	+9	+37	−8	+1	−146	−45	10
51209.697	0.871	+124	−16	−325	+5	+2	+132	−6	−2	−310	+7	10
51210.850	0.061			−47	−4	−17	+9	−7	+1			10
51211.825	0.221	−124	−5	+240	+10	+7	−107	−5	−4	+225	−17	10
51215.867	0.886	+158	+9	−346	+4	+3	+154	+9	+11	−332	+3	10
51216.746	0.030	+90	+26	−171	−4	−17	+77	+10	+16	−152	0	10
51217.870	0.215	−99	+19	+229	+1	−3	−93	+9	+10	+236	−4	10
51218.822	0.372			+195	−3	−7	−77	+11	+13	+208	−1	10

Note: $(O-C)_1$, $(O-C)_2$ and $(O-C)_3$ refer to the solutions for He I, He II and 'Combined', presented in Table 4 and Figs 3 and 4.

performed an orbital solution combining the radial velocities of He II 4686 Å and He I 4471 Å for the primary and secondary components, respectively. This solution is presented in Table 4 in the column labelled as *combined* and in Fig. 4. Previous published solutions obtained by CW76 and SL93 are also shown in the same table for comparison.

4.2 The period of apsidal motion

An inspection of the new data suggests a somewhat lower eccentricity and a considerably larger value of the longitude of periastron ω than those found in previous solutions. While the lower eccentricity probably originates in a better phase coverage of

our observations, the change in ω must be caused by apsidal motion (as first suggested by SL93). Consequently, we decided to investigate the hypothesis of apsidal motion, calculating orbital solutions for each individual radial velocity data set obtained over the years since the first determination by CW76. We used the radial velocity data for the primary component only, and adopted for the orbital period and eccentricity our best estimates of $P = 6.0803$ d and $e = 0.37$. Table 5 presents the resulting ω for the corresponding data sets. The variation of ω as a function of time is represented in Fig. 5 along with the obtained least-squares linear fit to those data, yielding an apsidal motion rate of $\dot\omega = 0°0324 \pm 0°0031$ per cycle, which corresponds to a period of 185 ± 16 yr. The ratio of apsidal to orbital motion ($\sim 10\,000$) is of the same order as observed for other massive binary systems, e.g. ι Ori (Marchenko et al. 2000), EM Car (Andersen & Clausen 1989), AO Cas (Monet 1980). Assuming for the HD 93205 binary system a total mass of the order of $100\,M_\odot$, which seems reasonable considering the spectral types of the components, the expected

relativistic contribution to the apsidal motion would be (following Batten 1973) close to $\dot\omega = 0°004$ per cycle. As the observed value is almost 10 times larger, we conclude that the apsidal motion of HD 93205 cannot be accounted for by relativistic effects. Tidal and rotational distortions must be the main cause of the apsidal motion in this binary. The possibility that this effect is partially caused by interaction with a third body in the system cannot be ruled out. If present, however, such a third body should probably be massive enough to be detected spectroscopically, which is not the case.

4.3 The mass ratio q and the spectral classifications of the binary components

We now consider the mass ratio (q). Our new value confirms those obtained in previous investigations, as seen from the coincidence

Figure 1. Rectified spectrograms of HD 93205 in the region of the He I 4471-Å (left) and He II 4686-Å (right) absorption lines at four orbital phases. 'P' and 'S' tick marks show the expected radial velocities for both binary components.
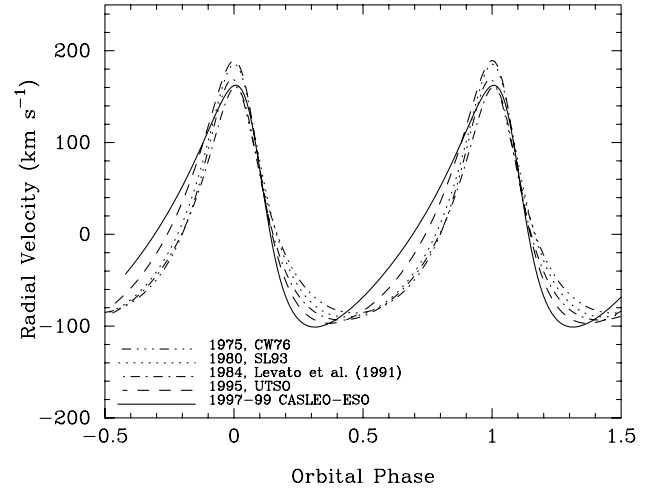

Figure 2. Best fits to radial velocities of the primary star in HD 93205 at different epochs to display the change of shape of the radial velocity curve. Solutions were derived adopting $P = 6^{\mathrm{d}}0803$ and a fixed eccentricity $e = 0.37$. Different radial velocity curves are shifted in phase to put all radial velocity maxima in phase $\phi = 0^{\mathrm{p}}.0$. All curves have been shifted to the same systemic velocity. Sources are identified according to the epoch of observations and authors.

Table 4. Orbital elements of HD 93205 binary components derived from radial velocities obtained in high-resolution spectrograms.

	He I 4471 Å	He II 4686 Å	Combined	CW76	SL93
$a_1 \sin i$ [km]	$(1.12 \pm 0.02)\,10^7$	$(1.03 \pm 0.02)\,10^7$	$(1.03 \pm 0.02)\,10^7$	$(1.015 \pm 0.047)\,10^7$	$(1.071 \pm 0.021)\,10^7$
$a_2 \sin i$ [km]	$(2.43 \pm 0.03)\,10^7$	$(2.41 \pm 0.02)\,10^7$	$(2.44 \pm 0.02)\,10^7$		$(2.457 \pm 0.077)\,10^7$
K_1 [km s^{-1}]	144.5 ± 2.6	131.5 ± 2.3	132.6 ± 2.0	139.1 ± 6.0	141.9 ± 3.0
K_2 [km s^{-1}]	312.1 ± 2.5	308.3 ± 2.3	313.6 ± 1.8	360 ± 53	324.8 ± 10.3
P [days]	6.0803 ± 0.0004	6.0803 ± 0.0004	6.0803 ± 0.0004	6.08102 ± 0.00066	6.08205 ± 0.00033
e	0.37 ± 0.01	0.35 ± 0.01	0.370 ± 0.005	0.49 ± 0.03	0.436 ± 0.016
ω [degrees]	52.0 ± 1.3	55.7 ± 1.4	50.8 ± 0.9	12 ± 3	16.3 ± 1.8
T_0 [+2,400,000 HJD]	50499.112 ± 0.017	50499.138 ± 0.017	50499.089 ± 0.012	42532.784 ± 0.060	44113.818 ± 0.02
T_{Vmax}	50498.702 ± 0.017	50498.679 ± 0.017	50498.695 ± 0.012		
γ [km s^{-1}]	-8.8 ± 1.3	2.2 ± 1.1	-2.9 ± 0.9	3.6 ± 2.5	30.2 ± 1.8
$M_1 \sin^3 i$ [M$_\odot$]	33.0 ± 1.6	30.8 ± 1.3	31.5 ± 1.1	39	32.6 ± 2.6
$M_2 \sin^3 i$ [M$_\odot$]	15.3 ± 1.5	13.1 ± 1.1	13.3 ± 1.1	15	14.2 ± 0.9
$q(M_2 M_1)$	0.463 ± 0.012	0.430 ± 0.010	0.423 ± 0.009	0.385 ± 0.090	0.437 ± 0.009
$P.E.$ [km s^{-1}]	11.4	8.6	8.4		

Notes: T_{Vmax} means the time of maximum radial velocity of the primary component. $P.E.$ represents the probable error of the fit.
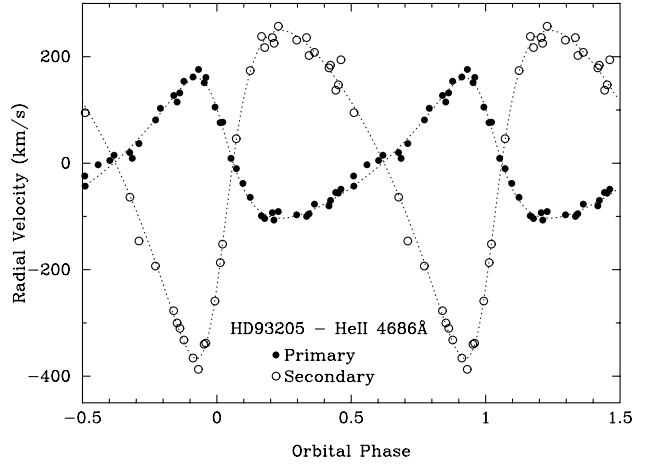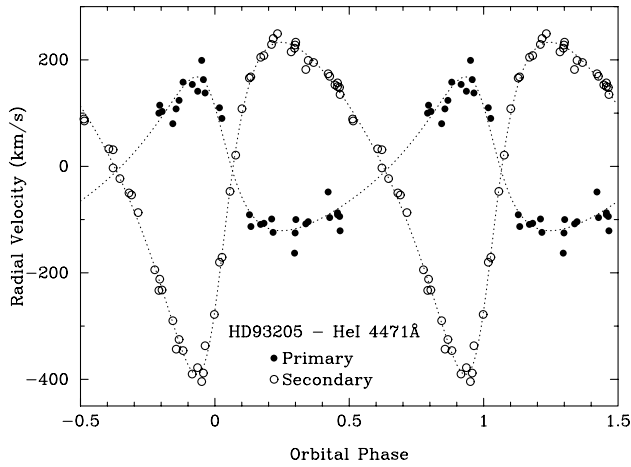
© 2001 RAS, MNRAS **326**, 85–94

Figure 3. Left: observed radial velocity for the primary (filled circles) and secondary (open circles) components of HD 93205 derived from the He I 44710-Å absorption line. Right: Observed radial velocity for the primary (filled circles) and secondary (open circles) components of HD 93205 derived from the He II 4686-Å absorption line.
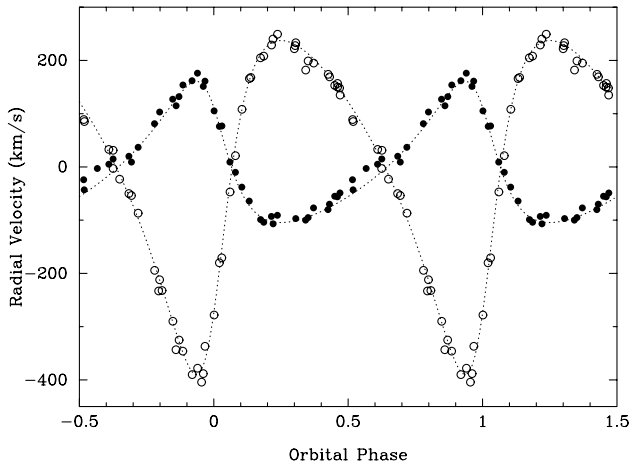

Figure 4. The spectroscopic orbit of HD 93205 computed from He II 4686-Å radial velocities for the primary component (filled circles) and He I 4471 Å for the secondary component (open circles). This radial velocity curve is labelled as the *combined* solution in Table 4.

Table 5. Longitude of periastrom derived from different radial velocity data sets.

Data set	T [HJD]	$\pm \Delta T$	ω [degrees]
Conti & Walborn (1976)	2 442 321	214	5.7 ± 6.1
Stickland & Lloyd (1993)	2 444 319	511	15.8 ± 4.7
Levato et al. (1991)	2 445 783	5	20.3 ± 14.8
Run 2	2 449 740	6	37.0 ± 12.0
Runs 3, 5, 9, 10	2 450 847	322	50.6 ± 0.9

Note: ΔT stands for the duration, counted from T, from the beginning and to the end of each data set.

(within the corresponding error bars) of the derived radial velocity semi-amplitudes for both components. As pointed out by Penny et al. (1998), the mass ratio of HD 93205 is the most problematic parameter for this binary system because it results in a surprisingly low mass of 51–58 $M_\odot$ for the primary O3 component when a reasonable value (around 22–25 $M_\odot$) is adopted for the secondary
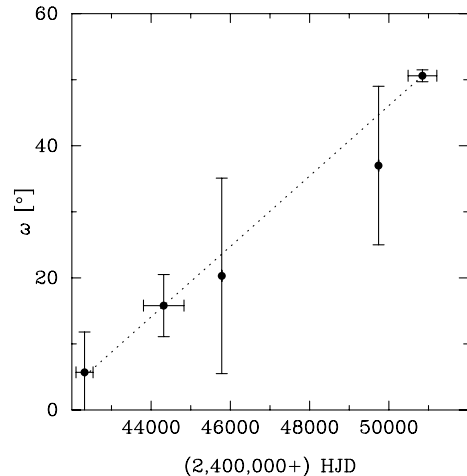

Figure 5. Variation of longitude of periastron (ω) as a function of time. Horizontal error bars show the time elapsed for each data set. Vertical error bars correspond to the errors obtained for each ω considering a fixed eccentricity ($e = 0.37$) derived in the orbital solution from radial velocities measured in our high-resolution spectrograms. The dotted line is the least-squares fitting with a slope of $0°.00533 \pm 0°.00051$ per day ($0°.0324 \pm 0°.0031$ per orbital cycle).

O8 component (in such a case the orbital inclination would be 57°–54°, thus excluding the possibility of detecting photometric variations resulting from eclipses, as also pointed out by Antokhina et al. 2000). The suggestion by SL93 that a somewhat earlier spectral type for the secondary component would help to solve this problem is ruled out by Penny et al. (1998) and also by a careful analysis of our high-resolution data. In fact, we inspected each échelle observation in our data set looking for changes in the spectral types of the binary components. For the secondary component, we confirm the O8 V spectral classification assigned since the beginning by CW76, even though slight changes, the phase-dependence of which is unclear, might occur (as can be barely seen in Fig. 1). Those changes could be related to the Struve–Sahade effect (Howarth et al. 1997) but, because the lines of the secondary component are considerably affected by dilution from the higher continuum of the primary component, their S/N in
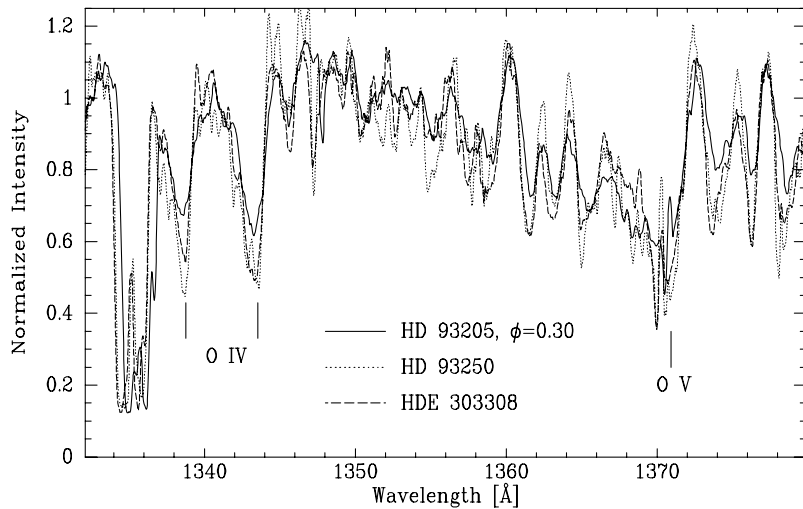
Figure 6. Portion of *IUE* spectra of HD 93205 (at orbital phase $\phi = 0.3$, full line), HD 93250 (dotted line) and HDE 303308 (dashed line). Note that the O v 1371-Å wind profile is very similar in all three stars, but the O IV doublet is weaker in HD 93205, supporting the O3 classification for the primary component.

our data is not high enough to ensure the detection of equivalent width variations. Consequently, we are persuaded to keep the O8 V spectral classification as most representative of the secondary component of the HD 93205 system.

Regarding the primary O3 V star, we notice that He I 4471 Å is present in its spectrum, but, as pointed out by Walborn (private communication) this fact does not suffice to assign a cooler spectral type to the star, because faint He I lines are also present on spectra of other O3 stars, for instance HDE 303308 observed with the same instrumental set-up, a fact also mentioned by Walborn & Fitzpatrick (1990).

We also searched the *IUE* data base and retrieved all the available observations of HD 93205, along with those corresponding to HDE 303308, HD 93250, HD 46223 and HD 96715 presented as O3 V((f)) and O4 V((f)) prototypes in the atlas of ultraviolet spectra by Walborn, Nichols-Bohlin & Panek (1985). A thorough comparison between these ultraviolet spectra showed that the ratio of the stellar wind profile of O v1371 Å to the O IV doublet at 1339–1343Å is even higher in the spectrum of the primary component of HD 93205 than in the spectra of HDE 303308 and HD 93250, both classified as O3 V((f)) (see Fig. 6). Since this ratio is definitely higher for the O3 V than the O4 V standard stars (see Walborn et al. 1985) we conclude that it brings more evidence in support of the classification of the primary component of HD 93205 as O3 V.

We also noticed that the feature at 1751 Å does not share the binary motion of HD 93205; thus, it is probably dominated by an interstellar line that blends with the N III 1751-Å absorption line, used in the above-mentioned atlas as a discriminant between spectral types O3 and O4. This feature was latter identified as interstellar Ni II 1751.9 Å by Walborn (private communication) who also finds that both 1748 Å and 1752 Å N III lines are weaker in the O3 spectrum than in other O-type stars, then allowing the interstellar Ni II line to dominate.

After reviewing the spectral classification of the binary components of HD 93205 we confirm, based on all the available material, the spectral types of O3 V and O8 V assigned earlier, with the suspicion of slight variations not larger than one subclass in the secondary spectrum. This leaves us again with the problem of explaining a mass ratio incompatible with present stellar evolutionary models (e.g. Schaller et al. 1992).

4.4 Position of the binary components in the Hertzsprung–Russell diagram

Once the spectral classification of the binary components is confirmed, we can use the photometric information in order to place HD 93205 on a theoretical Hertzprung–Russell Diagram (HRD), M_{bol} versus $\log T_{eff}$. We adopt for HD 93205 the distance modulus obtained by Massey & Johnson (1993) for Trumpler 16 ($V_0 - M_V = 12.55$). These authors give for HD 93205 an intrinsic visual magnitude $V_0 = 6.48$ [using $E(B - V) = 0.40$ and $R = 3.2$]. In order to derive individual bolometric magnitudes, we need an estimate of the visual luminosity ratio of the binary components. The luminosity ratio was determined through Petrie's method as described by Niemela & Morrison (1988). Petrie (1940) demonstrated that the luminosity ratio can be determined through the ratio of the equivalent widths (*EW*) of well separated spectral lines in the binary components, compared with *EW* of single stars of the same spectral types. In order to apply this method, we measured *EW* of He II 4686 Å, 4542 Å, and He I 4471 Å in several échelle observations at maximum radial velocity separation (near phases $0^p.0$ and $0^p.3$) for both binary components of HD 93205, and also we performed similar measurements on spectra of HD 93250, [O3 V(f)] and Tr16-22 (O8 V) obtained for comparison at CASLEO with the same instrumental configuration. These *EW* have typical errors ranging from 0.03 to 0.05 Å. A summary of the measured *EW*s is presented in Table 6, along with *EW* determination from Mathys (1988) for HD 93250 and HD73882 (O8 V). With this information we derived luminosity ratios, $L(O8 V)/L(O3 V)$ of 0.47 ± 0.22, 0.24 ± 0.06, and 0.22 ± 0.06, using He I 4471 Å, He II 4542 Å and He II 4686 Å, respectively. The large relative error in the luminosity ratio derived from the *EW* of He I 4471 Å originates in the faintness of this line in the O3 V spectrum. We then decided to adopt for the luminosity ratio of the binary components in HD 93205 the average of the ratios obtained from the two He II lines, namely 0.23 ± 0.06. This value is lower than 0.4 determined by Howarth et al. (1997) from cross-correlation of *IUE* data and also lower than 0.33 visually estimated by CW76 from photographic spectra.

With the above determined luminosity ratio, we obtained $V_0 = 6.70$ for the primary and $V_0 = 8.30$ for the secondary, resulting in visual absolute magnitudes M_V of -5.87 and -4.32

Table 6. Equivalent width measurements.

Star	ST	He I 4471	He II 4542	He II 4686	References
HD 73882	O8 V	0.62	0.45	0.55	1
HD 93250	O3 V(f)	0.07	0.68	0.54	1
		0.12 ± 0.03	0.68 ± 0.04	0.58 ± 0.03	2
Tr16−22	O8 V	0.65 ± 0.05	0.49 ± 0.03	0.54 ± 0.03	2
HD 93205 Prim.	O3 V	0.07 ± 0.02	0.63 ± 0.04	0.54 ± 0.03	2
1.25cm Sec.	O8 V	0.18 ± 0.03	0.11 ± 0.03	0.11 ± 0.03	2

(1). Mathys (1988).
(2). This paper.

respectively. With T_{eff}, and bolometric corrections (BC) corresponding to the spectral types (Vacca, Garmany & Shull 1996), we get $M_{bol}(O3V) = -10.41$ and $M_{bol}(O8V) = -7.87$, and $\log T_{eff}(O3V) = 4.71$ and $\log T_{eff}(O8V) = 4.58$, which places the binary components of HD 93205 very near the evolutionary tracks of an 85-$M_\odot$ ZAMS star and a 27-$M_\odot$ star (slightly above the ZAMS) respectively, according to Schaller et al. (1992). The calibration of T_{eff} and BC of Schmidt-Kaler (1982) would place the binary components on the evolutionary tracks corresponding to 100 $M_\odot$ and 25 $M_\odot$, respectively. These results are obviously inconsistent with the observed mass ratio. No matter which calibration we choose, the O8 V component appears near the evolutionary track of a 25-$M_\odot$ star, showing quite good agreement between masses derived through the observation of eclipsing binary systems and numerical evolutionary models of single stars, while the O3 V star will always appear above the 85-$M_\odot$ track, a value considerably higher than those corresponding to the observed mass ratio ($q = 0.42$), which would imply 52–60 $M_\odot$.

5 THE X-RAY LIGHT CURVE OF HD 93205

As HD 93205 is an eccentric binary with a massive companion, it is a good candidate to show X-ray emission resulting from wind–wind collisions (in addition to intrinsic emission which may be associated with instabilities in the winds of each star). In a massive binary, the wind from the primary star collides with the wind or surface of the companion, producing hot shocked gas which emits thermal X-rays. In an adiabatic shock, the X-ray luminosity varies as $1/D$ (Stevens, Blondin & Pollock 1992; Usov 1992), where D is the separation between the two stars. An eccentric binary like HD 93205 should also show phase-locked emission variations in which the X-ray flux is maximum at periastron and minimum at apastron (though in systems in which the colliding wind shock is eclipsed by the stellar wind, the observed flux variations are modulated by wind absorption). For HD 93205, $e = 0.37$, so that the expected ratio of the flux at periastron to the flux at apastron is $f_{peri}/f_{ap} \approx (1 + e)/(1 - e) \approx 2.2$. The actual variation may be smaller than this because of contamination by X-ray emission intrinsic to the winds of the component stars.

ROSAT PSPC observations (Corcoran et al. 1995) clearly showed that HD 93205 is a significant X-ray source, though in the PSPC image HD 93205 is blended with emission from HD 93204, which lies about 20 arcsec to the southwest. A deep *ROSAT* HRI pointing obtained by the X-Mega group resolved the emission from HD 93205 and HD 93204, and showed that HD 93204 is about 30 per cent fainter in the *ROSAT* band than HD 93205. In the resolved HRI image, the average net count rate of HD 93205 is about 0.012 HRI count s^{-1}. Assuming a Raymond–Smith type spectrum with $kT = 1.0$ keV and $N_H = 3 \times 10^{21}$ cm^{-2} (typical of other stars in the Carina Nebula), this corresponds to an observed flux of $3.2 \times$

Table 7. *ROSAT* observations of HD 93205 considered in the present analysis.

Sequence	Observer	Exposure Time (s)
rh150037n00	J. PULS	3352
rh202331n00	The XMEGA Group	47096
rh900385a02	J. SCHMITT	523
rh900385a03	J. SCHMITT	40556
rh900385n00	J. SCHMITT	11528
rh900644n00	M. CORCORAN	1721
rp200108n00	W. WALDRON	1610
rp201262n00	A. PAULDRACH	5665
rp900176a01	J. SWANK	14544
rp900176n00	J. SWANK	24321

10^{-13} erg cm^{-2} s^{-1} and an absorption-corrected flux of about 6×10^{-13} erg cm^{-2} s^{-1} in the broad *ROSAT* band, 0.2–2.4 keV. This corresponds to an unabsorbed luminosity $L_x = 8 \times 10^{32}$ erg s^{-1} assuming $V_0 - M_V = 12.55$. If the total system bolometric luminosity is $L_{bol} \approx 1.3 \times 10^6$ $L_\odot$, then $L_x/L_{bol} \approx 10^{-7}$, similar to the ratio for single O stars. Thus the average luminosity shows no clear evidence of excess X-ray emission produced by wind–wind collisions.

Another indication of the importance of colliding-wind emission is X-ray source variability, because single O stars in general do not vary greatly (Berghoefer et al. 1997), while colliding wind sources should show phase-dependent X-ray variations. A *ROSAT* PSPC light curve of the star was obtained by Corcoran (1996), but this light curve showed little significant variability. Much more X-ray data is currently available in the *ROSAT* archives, so, in order to re-examine whether HD 93205 shows any phase-locked X-ray variability, we extracted X-ray light curves for HD 93205 from archived PSPC and HRI observations (excluding data sets in which HD 93205 was more than 20 arcmin from the centre of the *ROSAT* field, to avoid complications arising from to vignetting and blending with nearby sources). We used both PSPC and HRI pointings, because both instruments are somewhat complementary: the PSPC provides greater sensitivity, though the observations suffer more from contamination by HD 93204; the HRI has poorer sensitivity than the PSPC but does not suffer as much from source contamination. Table 7 lists the available *ROSAT* data we used (those beginning with 'rh' indicate HRI data, those with 'rp' PSPC data), the observer, and the exposure time in seconds.

For each data set we extracted source light curves in 512 second bins from a circular source region of about 45 arcsec radius for the PSPC and about 12 arcsec radius for the HRI centred on HD 93205. We extracted background light curves with the same time binning from an apparently blank circular region centered roughly between the X-ray sources η Carinae, WR 25, HD 93129 and HD 93250, of
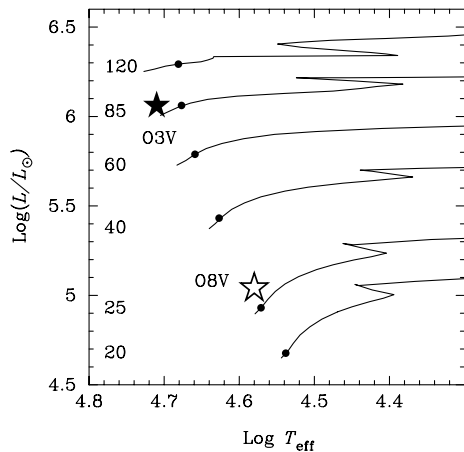
Figure 7. Hertzsprung–Russell diagram of the binary system HD 93205, representing the primary O3 V component with a black star, and the secondary O8 V with a white star. Continuous lines are solar metallicity evolutionary tracks from Schaller et al. (1992) and black dots a 10^6-year isochrone.
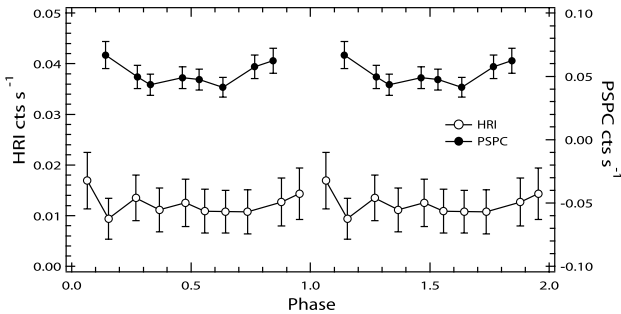

Figure 8. *ROSAT* PSPC and HRI light curves for HD 93205.

radius ≈ 1 arcmin. For each data set we generated background-subtracted source light curves, and then combined the data for each instrument individually and phase-averaged the resulting light curves using the 'combined' ephemeris given in Table 4. The resulting phase-averaged PSPC and HRI light curves are shown in Fig. 8. Both light curves indicate a rise in X-ray flux from HD 93205 near phase = 0, i.e. near periastron passage. Though the significance is not high, the similarity in phasing and amplitude of the HRI and PSPC light curves suggests that at least some of the X-ray emission from HD 93205 originates in the wind–wind collision between the O3 star and the O8 companion. The ratio of the PSPC rate near periastron ($\phi = 0.9$) to that at $\phi = 0.5$ is about 1.75. For the HRI light curve, the ratio of the flux at $\phi = 1.08$ to that near $\phi = 0.5$ is about 1.70. Both the PSPC and HRI light curves show a level of variability that is near that expected from a colliding wind model where the X-ray flux varies as the inverse of the stellar separation.

6   SUMMARY AND CONCLUSIONS

We have presented a new and improved determination of orbital elements for the HD 93205 binary system based on high-resolution CCD spectroscopy. Our radial velocity orbits yield semiamplitudes of $K_1 = 133 \, \mathrm{km \, s^{-1}}$ and $K_2 = 314 \, \mathrm{km \, s^{-1}}$ for the primary and secondary binary components, respectively. These values are in the range of the previous determinations (within the error bar

intervals), and therefore they confirm the mass ratio q of 0.42. We have revised the spectral classification of both binary components using our optical spectra and archive UV *IUE* observations, concluding that the O3 V + O8 V spectral types assigned by CW76 are appropriate, but not excluding the possibility of a slight 'Struve–Sahade effect' (as suggested by Howarth et al. 1997). The luminosity ratio of the binary components, estimated from our CCD spectra through Petrie's (1940) method, results in $L(O8V)/L(O3V) = 0.23$. Combining this luminosity ratio with the published photometry and $\log T_{\mathrm{eff}}$ and bolometric corrections derived from the spectral types, we place the binary components of HD 93205 on a theoretical HRD, finding that the O8 V component lies on the evolutionary track of a 25–$27 \, \mathrm{M_\odot}$ star, and the O3 V component lies between the tracks corresponding to 85–$100 \, \mathrm{M_\odot}$. This would result in a mass-ratio $q = 0.25$–0.32, in obvious disagreement with q determined from the radial velocity orbit.

From studies of massive binary systems it is well established that the mass of an O8 V star is close to 22–$25 \, \mathrm{M_\odot}$ (e.g. EM Car, Solivella & Niemela 1986; Andersen & Clausen 1989; HH Car, Mandrini et al. 1985; Schönberner & Harmanec 1995). Assuming this 'normal' value of ~ 22–$25 \, \mathrm{M_\odot}$ for the mass of the secondary component of HD 93205, we obtain, through the determined mass ratio, 52–$60 \, \mathrm{M_\odot}$ for the O3 V primary component, considerably below the mass value predicted by the evolutionary models. Since HD 93205 is the only double-lined binary system containing an O3 V component for which a radial velocity orbit is available at present, it is not possible to make any comparisons, but the lack of other mass determinations exceeding $60 \, \mathrm{M_\odot}$ and our estimate for the mass of the O3 V component just obtained seem to be significative clues indicating that the derivation of masses for hot stars based on the comparison of observed luminosities with numerical evolutionary tracks might lead to a significant overestimate. This seems to support the so-called 'mass discrepancy' between masses derived via evolutionary models and those inferred from observations (mainly spectroscopic), first studied by Herrero et al. (1992). In a recent paper, Herrero, Puls & Villamariz (2000) showed that this discrepancy (while solved for many cases with the use of new model atmospheres and evolutionary tracks) still holds for objects with low gravities, which is probably not the case for HD 93205. In another recent paper, Meynet & Maeder (2000) have analysed the effect of rotation on stellar evolutionay models. These authors state that, for the most part, the mass discrepancies for massive stars might be solved through the use of rotating models in the determination of the evolutionary masses. However, they find that the effect of rotation should be negligible for objects with high gravities (and therefore early evolutionary stage). This is probably the case for HD 93205, which is a member of a very young open cluster and does not exhibit traces of evolution in its spectrum (for example, He II 4686 Å is seen as a deep absorption, as in stars near the zero-age main sequence). Moreover, the projected rotational velocities of HD 93205, as found by Howarth et al. (1997), are $135 \, \mathrm{km \, s^{-1}}$ and $145 \, \mathrm{km \, s^{-1}}$ for primary and secondary, respectively. With an inclination of $54°$–$57°$ the actual rotational velocity of the primary component would be 161–$167 \, \mathrm{km \, s^{-1}}$, which is not a very large value.

The Carina Nebula, where HD 93205 is immersed, harbours many massive binaries. Among them we mention WR 22, a remarkable Wolf–Rayet binary system containing the most massive WR star known at present in a binary. Recently, Schweickhardt et al. (1999) derived masses of $55 \pm 7 \, \mathrm{M_\odot}$ and

$21 \pm 2\,\mathrm{M}_\odot$ for the WN7ha and O8–O9.5 III–V binary components of WR 22. The similarity between these mass values and those estimated for HD 93205 is so striking that we wonder whether both systems represent somewhat different evolutionary stages of the same kind of massive binary systems. Even nearby η Carinæ may be a binary with components of 'only' $\sim 70 + 70\,\mathrm{M}_\odot$ (Damineli, Conti & Lopes 1997). While the final jury is still out, we suspect that well-separated, unevolved binaries like HD 93205 provide the most reliable technique for determining stellar masses, relying on a minimum of assumptions compared with most other techniques. Hence, we are led to speculate that there are still serious problems of overestimation of the masses of massive stars, based on both evolutionary and spectroscopic methods derived other than from Keplerian orbits, which become progressively worse for the higher masses.

We have also found that HD 93205 presents fast apsidal rotation with a period of 185 ± 16 yr, mainly owing to tidal forces. In a forthcoming paper (Benvenuto et al., in preparation) we will try to use this new determination to find an independent estimate of the masses of the binary components of HD 93205.

While the total X-ray emission of HD 93205 results in a ratio $L_\mathrm{x}/L_\mathrm{bol}$ simlar to that observed in other O-type stars, the X-ray light curve shows a rise in X-ray flux near periastron passage probably arising from wind–wind collision effects. This effect is present in both PSPC and HRI light curves, and the observed ratio of the flux at periastron to the flux at apastron is about 1.7.

ACKNOWLEDGMENTS

REFERENCES

Albacete Colombo J. F., Morrell N., Niemela V., 2001, MNRAS, 326, 78 (Paper 1, this issue)
Andersen J., Clausen J. V., 1989, A&A, 213, 183
Antokhina E. A., Moffat A. F. J., Antokhin I. I., Bertrand J.-F., Lamontagne R., 2000, ApJ, 529, 463
Batten A. H., 1973, Binary and Multiple Systems of Stars. Pergamon Press, Braunschweig, p. 127
Benvenuto O. G., Serenelli A. M., Althaus L. G., Barbá R. H., Morell N. I., 2001, MNRAS, submitted
Berghoefer T. W., Schmitt J. H. M. M., Danner R., Cassinelli J. P., 1997, A&A, 322, 167
Bertiau F. C., Grobben J., 1969, Ric. Astron. Sp. Vaticana, 8, 1
Bertrand J.-F., Sr-Louis N., Moffat A. F. J., 1998, in Howarth I., ed., ASP Conf. Ser. Vol. 131, Boulder-Munich II: Properties of Hot, Luminous Stars. Astron. Soc. Pac., San Francisco, p. 376
Burkholder V., Massey P., Morrell N. I., 1997, ApJ, 490, 328
Cincotta P. M., Méndez M., Núñez J. A., 1995, ApJ, 449, 231
Conti P. S., Walborn N. R., 1976, ApJ, 207, 502 (CW76)
Corcoran M. F., 1996, Rev. Mex. Astron. Astrofis., Ser. Conf., 5, 54
Corcoran M. F., 1999, Rev. Mex. Astron. Astrofis., Ser. Conf., 8, 131
Corcoran M. F., Swank J., Rawley G., Petre R., Schmitt J., Day C., 1995, Rev. Mex. Astron. Astrofis., Ser. Conf., 2, 97
Corcoran M. F. et al. (the XMEGA group), 1999, in van der Hucht K. A., Koenigsberger G., Eenens P. R. J., eds, IAU Symp. 193: Wolf–Rayet Phenomena in Massive Stars and Starburst Galaxies. Astron. Soc. Pac., Chelsea, p. 772
Damineli A., Conti P. S., Lopes D. F., 1997, New Astron., 2, 107
García B., Malaroda S., Levato H., Morrell N. I., Grosso M., 1998, PASP, 110, 53
Garmany C. D., Conti P. S., Massey P., 1980, ApJ, 242, 1063
Herrero A., Kudritzki R. P., Vilchez J. M., Kunze D., Butler K., Haser S., 1992, A&A, 261, 209
Herrero A., Puls J., Villamariz M. R., 2000, A&A, 354, 193
Howarth I. D., Siebert K. W., Hussain G. A. J., Prinja R. K., 1997, MNRAS, 284, 265
Lafler J., Kinman T. D., 1965, ApJS, 11, 199
Levato H., Malaroda S., Morrell N., García B., Hernández C., 1991, ApJS, 75, 869
Mandrini C. H., Méndez R. H., Ferrer O. E., Niemela V. S., 1985, Rev. Mex. Astron. Astrofis., 11, 99
Marchenko S. et al., 2000, MNRAS, 317, 333
Massey P., Hunter D. A., 1998, ApJ, 493, 180
Massey P., Johnson J., 1993, AJ, 105, 980
Mathys G., 1988, A&AS, 76, 427
Meynet G., Maeder A., 2000, A&A, 361, 159
Monet D. G., 1980, ApJ, 237, 513
Niemela V. S., Morrison N. D., 1988, PASP, 100, 1436
Penny L. R., Gies D. R., Hartkopf W. I., Mason B. D., Turner N. H., 1993, PASP, 105, 588
Penny L. R., Gies D. R., Bagnuolo W. G., Jr, 1998, in Howarth I., ed., ASP Conf. Ser. Vol. 131, Boulder-Munich II: Properties of Hot, Luminous Stars. Astron. Soc. Pac., San Francisco, p. 392
Petrie R. M., 1940, Pub. DAO, 7, 205
Schaller G., Schaerer D., Meynet G., Maeder A., 1992, A&AS, 96, 269
Schmidt-Kaler Th., 1982, Landolt-Börnstein, NS, Vol. 2. 455
Schöenberner D., Harmanec P., 1995, A&A, 294, 509
Schweickhardt J., Schmutz W., Stahl O., Szeifert Th., Wolf B., 1999, A&A, 347, 127
Solivella G. R., Niemela V. S., 1986, PASP, 98, 788
Stevens I. R., Blondin J. M., Pollock A. M. T., 1992, ApJ, 386, 265
Stickland D. J., Lloyd C., 1993, Observatory, 113, 256 (SL93)
Usov V. V., 1992, ApJ, 389, 635
Vacca W. D., Garmany C. D., Shull J. M., 1996, ApJ, 460, 914
van Genderen A. M. et al., 1985a, A&A, 151, 349
van Genderen A. M. et al., 1985b, A&AS, 61, 213
van Genderen A. M. et al., 1989, A&AS, 79, 263
Walborn N. R., 1971, ApJ, 167, L31
Walborn N. R., 1973, ApJ, 179, 517
Walborn N. R., 1995, Rev. Mex. Astron. Astrofis., Ser. Conf., 2, 51
Walborn N. R., Fitzpatrick E. L., 1990, PASP, 102, 379
Walborn N. R., Nichols-Bohlin J., Panek R. J., 1985

This paper has been typeset from a TEX/LATEX file prepared by the author.